

## Solidification behavior of undercooled Ni-Pb hypermonotectic alloy

H. XIE, G. C. YANG, W. X. HAO, J. F. FAN

State Key Laboratory of Solidification Processing, Northwestern Polytechnical University, Xi'an, Shaanxi 710072, People's Republic of China

Monotectic system alloys possess certain excellent physical and chemical properties, and they can be used as self-lubricating materials, electrical contact materials, superconducting materials and so on [1, 2]. However, it is very difficult to prepare immiscible hypermonotectic alloys with homogeneous structures by employing conventional casting, because the parent liquid will decompose into two distinct immiscible liquids in a few seconds when it passes through the immiscibility gap [3–5]. In the past several decades, the development of aerospace science and technology aroused fresh interest in studying solidification behavior of hypermonotectic alloys, but there are still some problems which have not been solved [6–8]. High undercooling technique can make bulk metal melts solidify at a high speed under large undercooling and produce homogeneous microstructure with almost no solution segregation [9, 10]. Therefore, the aim of our present work is to undercool Ni-20 at.%Pb hypermonotectic alloy to a significant extent and to investigate its solidification behavior over a large range of undercooling.

The experiments were performed by the method of molten glass fluxing and recycle superheating with a high-frequency induction furnace. The samples were prepared by *in-situ* alloying procedure from 99.99% pure Ni and 99.75% pure Pb. After grinding off the surface oxide and etching in HCl solution diluted by alcohol, the alloy charge was immersed into a pool of molten glass in a quartz crucible, was melted and superheated to 1923 K which is above the consolute temperature (1773 K) of the immiscibility gap to ensure homogeneous alloying. The superheating time was 3–5 min. Several superheating cycles were conducted till the undercooling became stable, and subsequently nucleation was stimulated at the predetermined undercooling using a nickel needle. The thermal behavior of samples was monitored by using an infrared pyrometer, which was calibrated with a standard PtRh30-PtRh60 thermocouple, and possessed a relative accuracy of 5 K and a response time less than 1 ms. Each of the samples had a mass of 6–8 g and a diameter of 12 mm, and was sectioned through the triggering spot, then polished, and etched with 8 g FeCl<sub>3</sub> + 20 ml HCl + 100 ml H<sub>2</sub>O solution. Structure observation was completed by using a Nephot-1 optical microscope and Amray-1000B SEM.

A large undercooling range from 182 to 418 K was obtained in this work. Optical micrographs illustrating the characteristics of the Ni-20 at.%Pb alloy are presented in Fig. 1.

Fig. 1a shows the microstructure of the sample undercooled by 182 K, which is composed of  $\alpha$ -Ni dendrites

and interdendrite massive Pb lumps. For the smaller undercooling range, the morphology character of  $\alpha$ -Ni is still typically dendritic and very rough, which is due to the small quantity of latent heat released during the course of recalescence [11]. In addition, the Pb lumps in the interdendrite spacing are very rough too and are undoubtedly caused by the coalescence of  $L_2$  (Pb) droplets which are rejected and pushed together by the overspreading dendrites. Where do the Pb lumps come from? They are mainly composed of both  $L_2$  phase separated from the parent liquid through the immiscible gap and  $L_2$  phase produced through the monotectic transformation. In the previous works, there is no obvious evidence achieved to describe liquid separation from the parent liquid through the immiscible gap under the condition of high undercooling. Fig. 2 presents the evidence of liquid-liquid separation achieved by water quenching at 1650 K and proves liquid-liquid separation to have occurred, in which the black, spherical Pb-rich droplet is surrounded by the white  $\alpha$ -Ni solid solution phase grown in the radial manner. In the case of separation of  $L_2$  droplets from the parent liquid, they grow and deposit, and  $\alpha$ -Ni dendrites formed behind the  $L_2$  phase affect the distribution of  $L_2$  phase by pushing  $L_2$  droplets together in the interdendrite spacing to form the Pb lumps.

Fig. 1b and c also show the distribution of Pb and the structure morphology of  $\alpha$ -Ni dendrites in which the undercooling is 242 and 378 K respectively. Compared with Fig. 1a, the sizes of Pb lumps are similar and the quantity of the lumps increases, which is caused by the large undercooling facilitating the coarsening of the Pb droplets [12, 13].

When the undercooling exceeds 378 K, the main feature of structure is the formation of anomalous granular grains in addition to the interdendritic lumps Pb and interdendritic Pb particles. Fig. 3 shows the SEM result of the sample undercooled by 418 K. A comparison of Fig. 1d, Fig. 3 and Fig. 1a–c indicates that the large undercooling is helpful to facilitate the fracture of the dendritic framework and the partial transferring of the Pb distribution from the interdendritic region to the intradendritic region.

Usually, the fracture of the dendritic framework can be explained by recrystallization mechanism of grain refinement [14, 15]. Under the conditions of large undercooling, dendrite remelting cannot really cause anomalous granular grains to form, because a large amount of heat has been released during the cooling course and the recalescence superheating of  $\alpha$ -Ni dendrites is in a smaller range. However, under

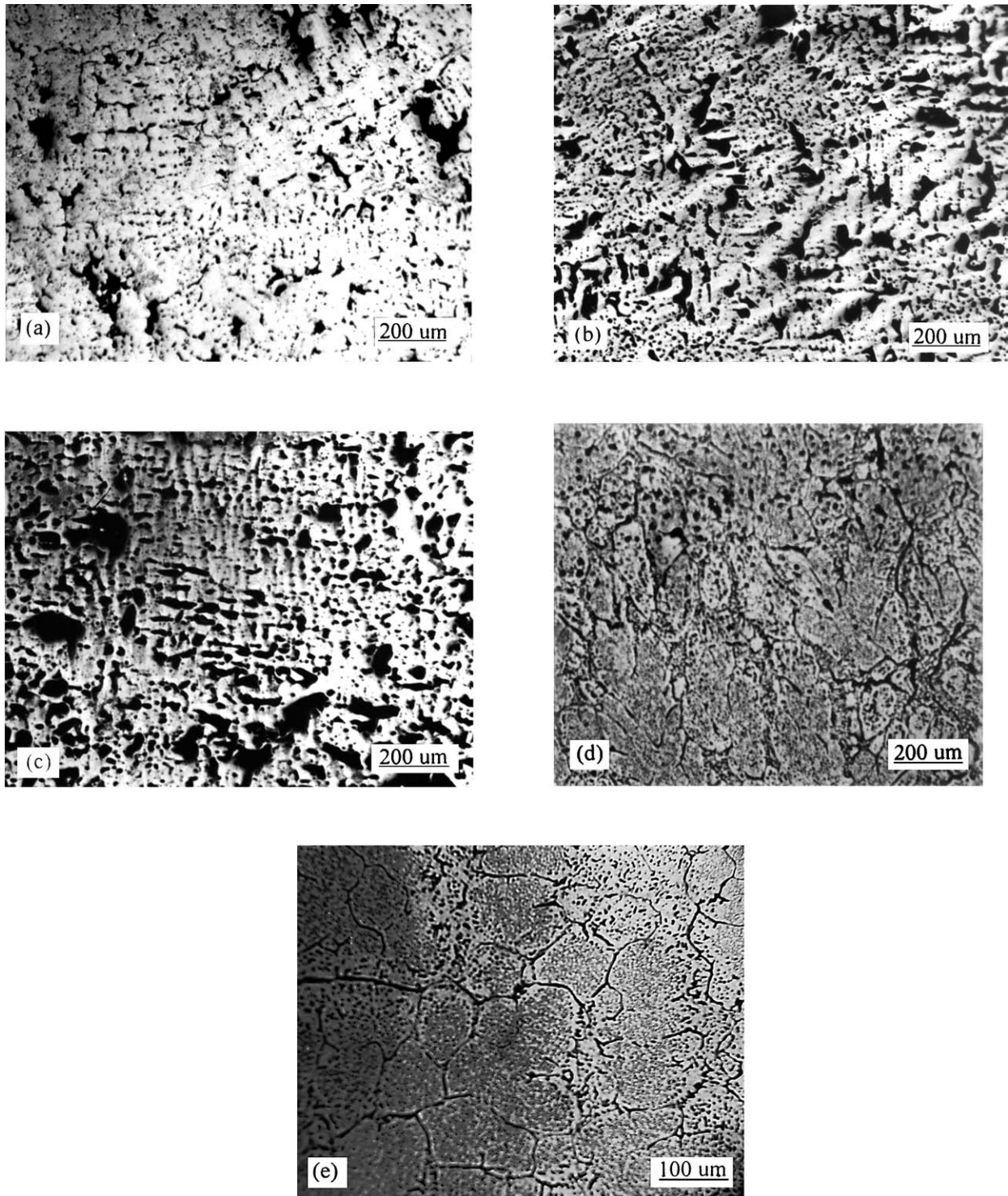


Figure 1 Microstructures of Ni-20 at.%Pb hypermonotectic alloy undercooled by (a)  $\Delta T = 182$  K, (b)  $\Delta T = 242$  K, (c)  $\Delta T = 378$  K, and (d)  $\Delta T = 418$  K ((e): (d) magnified).

the conditions of large undercooling, higher dendritic growth velocity of  $\alpha$ -Ni causes the inner stress to increase because of the unbalanced shrinkage of  $\alpha$ -Ni solid solution phase. In addition, the dendrite defects also increase strikingly with increase of the growth velocity. Finally driven by interfacial energy, recrystallization takes place and causes anomalous grains to form [15].

The maximum solid solubility of Pb in  $\alpha$ -Ni, which is about 1.02 at.% (or 4.1 wt%) under equilibrium solidification conditions, was also investigated under conditions of high undercooling. Our present work reveals

the Pb solubility reaches 5.83 at.% (or 17.83 wt%) in the sample undercooled by 418 K. The intradendritic Pb particles in the SEM micrograph (see Fig. 3) are the products of distinct solution trapping by the advancing solid/liquid interface.

In summary, the structure morphology and the Pb distribution of the undercooled melt were investigated systematically by the method of glass fluxing and cyclic superheating. Ni-20 at.%Pb hypermonotectic alloy has been undercooled by amounts up to 418 K. The structure after lower undercooling of 182 K is composed of coarse  $\alpha$ -Ni dendrites and intradendritic massive Pb

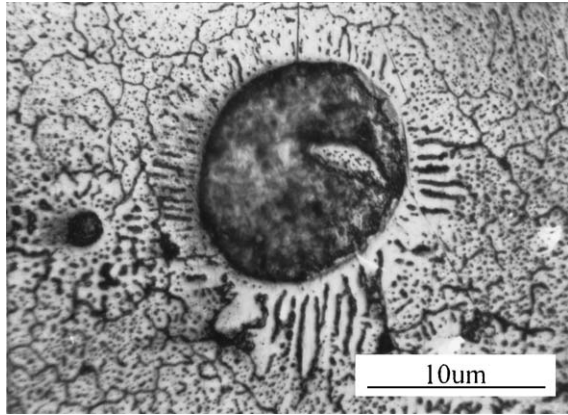


Figure 2 Liquid-liquid separations during the course of cooling through immiscible gap (quenched by water at 1650 K).

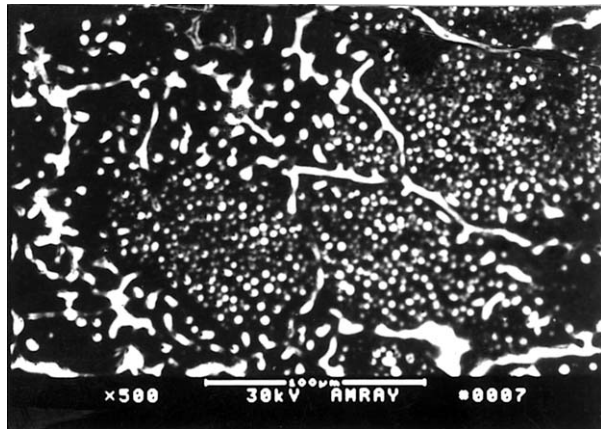


Figure 3 SEM image of Ni-20 at.%Pb alloy undercooled by 418 K.

lumps. Over the large undercooling range from 242 to 378 K, large undercooling facilitates liquid-liquid separation and causes  $\alpha$ -Ni dendrites to become fine. When

undercooling was increased to 418 K, the content of Pb increased to 5.83 at.% (or 17.83 wt%) for distinct solution trapping and the main structure feature of the sample was the formation of anomalous grains.

### Acknowledgments

The authors are grateful to the National Natural Science Foundation of China, grant no. 50171055, the Aviation Science Foundation of China, grant no. 01G53046, Shaanxi Natural Science Foundation, grant no. 2000C02 and the Doctorate Creation Foundation of NWPU, grant no. 200208 for the financial support.

### References

1. S. J. SVAGE and F. H. FORES, *J. Metals*, **36** (1984) 20.
2. H. GELLES and A. J. MARKWORTH, *J. AIAA*, **16** (1978) 431.
3. A. P. XIAN, H. W. ZHANG, *et al.*, *Acta Metall. Sinica*, **32** (1996) 113.
4. H. W. ZHANG and A. P. XIAN, *ibid.*, **35** (1999) 1187.
5. Y. LIU, J. J. GUO and J. JIA, *Foundry*, **49** (2000) 11.
6. W. H. TAIT, *The Iron and Steel Inst (Spec Rep)*, **38** (1947) 157.
7. K. UENISHI, *et al.*, *J. Mater. Sci.*, **29** (1994) 4860.
8. R. J. FEDER, *et al.*, US Patent no. 3797084 (1974).
9. J. F. LI, *et al.*, *Mater. Sci. Eng. A* **277** (2000) 161.
10. Z. Z. ZHANG, *et al.*, *Progr. Nat. Sci.*, **10** (2000) 364.
11. H. X. ZHENG, H. XIE and X. F. GUO, *The Chinese J. Nonferr. Met.*, **2** (2001) 265.
12. C. DONG and B. WEI, *J. Mater. Sci. Lett.*, **15** (1996) 970.
13. B. WEI, *et al.*, *Mater. Sci. Eng. A* **173** (1993) 357.
14. B. L. JONES and G. M. WESTON, *The J. Australian Inst. Met.*, **15** (1970) 167.
15. F. LIU, X. F. GUO and G. C. YANG, *J. Cryst. Growth*, **219** (2000) 489.

Received 2 May  
and accepted 24 October 2003